*Massive Stars Near and Far*
*Proceedings IAU Symposium No. 361, 2024*
*J. Mackey, J. S. Vink, & N. St-Louis, eds.*
doi:10.1017/S1743921322002502

# NGC 3125-A1 revisited at higher spectral resolution with COS G160M

**A. Wofford[1], A. Sixtos[1], L. Smith[2], S. Charlot[3] and G. Bruzual[4]**

[1]Instituto de Astronomía, Universidad Nacional Autónoma de México, Unidad Académica en Ensenada, Km 103 Carr. Tijuana-Ensenada, Ensenada 22860, México
email: awofford@astro.unam.mx

[2]Space Telescope Science Institute, 3700 San Martin Drive, Baltimore, MD 21218, USA

[3]Sorbonne Université, UPMC-CNRS, UMR7095, Institut d'Astrophysique de Paris, F-75014 Paris, France

[4]Instituto de Radioastronomía y Astrofísica, UNAM, Campus Morelia, Michoacán, C.P. 58089, México

**Abstract.** Super star cluster (SSC) A1 in starburst galaxy NGC 3125 has the strongest broad He II $\lambda$1640 emission line ever observed in the nearby Universe and constitutes an important template for interpreting observations of galaxies that are located out to a redshift of $z \sim 3$. We use observations of SSC A1 obtained with the Cosmic Origins Spectrograph (COS) on board of the Hubble Space Telescope (HST) in order to check if there is a contribution of nebular emission to the He II line. In addition, we compare the COS G130M + G160M observations of A1 ($1150 - 1750$ Å) to the latest Charlot & Bruzual population synthesis models, which account for Very Massive Stars (VMS) of up to 300 $M_{\odot}$. A model with $Z = 0.008$ and age = 2.4 Myr provides a very reasonable fit to the C III $\lambda$1175, N V $\lambda$1240, C IV $\lambda$1550, He II $\lambda$1640, and N IV $\lambda$1718 stellar-wind features, although the O V $\lambda$1371 line is not well reproduced. Overall, our results show the great improvement of stellar evolution and population synthesis models over the past decade, and in particular, the improved formulation of stellar mass loss rates.

**Keywords.** techniques: spectroscopic, galaxies: starburst, galaxies: stellar content, ultraviolet: stars

## 1. Introduction

Starburst galaxies are characterized by massive violent bursts of star formation. They are powered by populations of hot stars with progenitor masses of 5 $M_{\odot}$ and above. Locally, they are responsible for 20% of the entire high-mass star formation (Brinchmann *et al.* 2004). Nearby starburst galaxies are the most obvious local counterparts of the normal star-forming galaxies discovered at high redshift, in particular galaxies located at redshifts of $z \sim 2 - 3$, i.e., at the epoch of 'Cosmic Noon'. The latter epoch is ideal to examine the mechanisms of star formation as it is when galaxies formed about half of their current stellar mass. Composite spectra of Cosmic-Noon galaxies (e.g., Shapley *et al.* 2003; Saxena *et al.* 2020) provide a glimpse of the dominant stellar populations present in the early Universe.

Nearby ($D = 11.5$ Mpc) starburst galaxy NGC 3125 (Tol 3) is of particular importance for studies of galaxies at Cosmic Noon. The galaxy has an ionized-gas oxygen abundance of 12+log(O/H)=8.3 (Hadfield & Crowther 2006), i.e., similar to that of the Large Magellanic Cloud (LMC). It is dominated by two emission regions, A and B. Region A can be subdivided into UV-bright and highly extinguished components

A1 and A2, respectively. In (Wofford *et al.* 2014, W14), we present HST observations of A1 obtained by PI Leitherer using the following two spectrographs and configurations: i) Space Telescope Imaging Spectrograph (STIS), 2"-wide long slit, and G140L grating; and ii) COS, 2.5"-wide circular aperture, and G130M grating. The analysis of these data by W14 shows that the spectroscopically-derived mass of A1 ($1.7 \times 10^5\,M_\odot$) is of the same order of magnitude as the binary-corrected virial mass of cluster NGC 2070 in the LMC ($4.5 \times 10^5\,M_\odot$, which is consistent with the mass determined from photometry; Bosch *et al.* 2009). The STIS data also show that A1 is characterized by broad ($FWHM \approx 1200\,\mathrm{km\,s^{-1}}$) He II $\lambda$1640 emission with a large equivalent width ($EW = 7.1 \pm 0.4$ Å; revised to $\sim 5$ Å based on the higher SNR data of this work); and stellar O V $\lambda$1371 absorption. Broad ($FWHM \approx 1000\,\mathrm{km\,s^{-1}}$) He II emission suggests stellar winds as the formation mechanism. In order to produce detectable stellar He II emission, one or more of the following conditions must be met: the stars must be hot to doubly ionize He, the mass-loss rates must be high to produce dense winds, and He must be overabundant. Since classical Wolf-Rayet (WR) stars meet all three conditions, the presence of He II is generally thought to indicate the presence of WR stars. Note however that H-rich Very Massive Stars (VMS), which have masses of $M > 150\,M_\odot$, i.e., above the canonical upper mass limit of the stellar Initial Mass Function (IMF), have WR features, independent of He enrichment. In VMS, the reason for the increased $EW$ of the He II $\lambda$4686 stellar-wind line is almost certainly the proximity to the Eddington limit. This is shown in figure 10 of Vink *et al.* (2011), where one sees that increasing the Eddington factor theoretically increases the mass loss rate, and also empirically, the He II $EW$. He II $\lambda$1640 is the UV counterpart to the optical He II line and a similar increase of the $EW$ is expected for the UV line as well.

In W14, we rule out that the extraordinary He II emission and O V absorption of A1 are due to an extremely flat exponent of the upper IMF, and suggest that they originate in the winds of VMS. Such stars have been found in the core of NGC 2070, which is known as R136 and is $1 - 2.5$ Myr old (Brands *et al.* 2022). An example of a VMS is R136a3, which has an initial mass of $165 \pm 30$ and is classified as a hydrogen-rich WN5h star. An ultraviolet spectrum of this star, obtained with the Goddard High Resolution Spectrograph (GHRS, an instrument that is no longer on board of HST) is shown in figure 5 (top panel) of Crowther *et al.* (2010). Note the striking similarity between the GHRS spectrum of R136a3 and the COS spectrum of SSC A1, which we show in Figure 2.

NGC 3125 can be used as a template to interpret composite spectra of distant star-forming galaxies that show broad He II emission (Chandar *et al.* 2004). In composite spectra, the uncertainties in the redshifts of the galaxies that make up the spectrum contribute to the width of the composite He II line. There is however now strong evidence of the existence of broad He II emission at high-redshift is provided by the recent discovery, in a deep observation with the Very Large Telescope, of broad ($FWHM \approx 920\,\mathrm{km^{-1}}$) He II emission from a single non-lensed galaxy that is located at $z \sim 3$, and that is not an AGN (Cullen, private communication). In order to obtain the best possible interpretation of the latter and other distant systems, it is crucial to verify the hypothesis that there are VMS in NGC 3125-A1. This hypothesis can be tested by comparing the UV spectra of A1 with population synthesis models. Such models predict the photometric and spectroscopic properties of stellar systems.

## 2. Is the He II line purely stellar?

Prior to testing the VMS hypothesis, it is important to check if the integrated He II line of A1 has a contribution from nebular emission. For this purpose, COS G160M spectra of A1, with superior spectral resolution and SNR relative to the STIS data that we analyzed in W14, were obtained by PI Wofford. Two central wavelengths (1600 and

https://doi.org/10.1017/S1743921322002502 Published online by Cambridge University Press

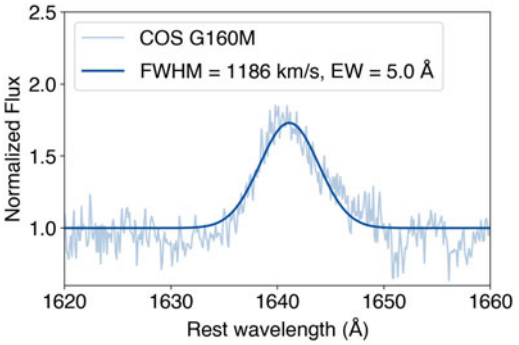


**Figure 1.** Portion of COS G160M spectrum of NGC 3125-A1 around He II $\lambda$1640 emission line (light blue curve) and Gaussian fit to the line (dark blue curve). The fit parameters are given in the legend.

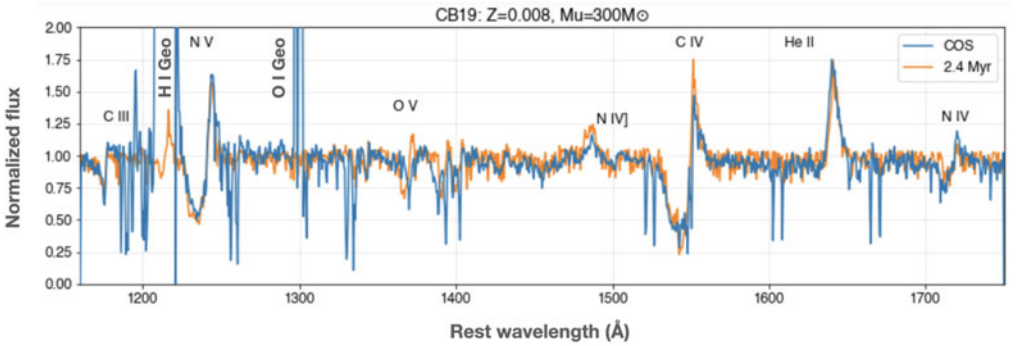


**Figure 2.** Comparison of COS G130M + COS G130M observation (blue curve) with best-fit model with VMS (orange curve). The strong emission lines at around 1210 and 1300 Å are due to Lyman-alpha and O I geocoronal emission.

1623 Å) were used in order to ensure continuous coverage in the wavelength range from $\sim$1400 to 1800 Å. A custom IDL program was used to co-add the exposures at the two central wavelengths. Figure 1 shows that the observed He II $\lambda$1640 emission line is purely stellar. The higher signal-to-noise in the continuum near the He II line of the G160M data relative to the STIS G140L observation enables a more accurate determination of the EW of the He II line. A Gaussian fit to the line in the G160M data yields $EW = 5\,\AA$ and $FWHM = 1186$ km s$^{-1}$. The lower value of the $EW$ obtained with the COS data relative to the STIS measurement is due to the better SNR in the nearby continuum of the COS observation, which enabled a more accurate fit to the line.

## 3. Preparation of spectrum for comparison with models

In order to prepare the COS observations for comparison with the models, we use custom programs that accomplish the following tasks: i) combine the G130M and G160M observations; normalize the spectrum by dividing it into sections that are normalized independently from each other (this is done by dividing each section by a straight-line fit to line-free portions within the section); iii) fit Voigt profiles to the Lyman-alpha aborption lines from the Milky Way and NGC 3125, after masking the nearby absorption or emission lines; iv) correct for the Lyman-alpha absorption lines; v) correct the spectrum

https://doi.org/10.1017/S1743921322002502 Published online by Cambridge University Press

for redshift; vi) degrade the observations to match the model spectral resolution. The observations cover the rest-frame UV wavelength range from 1150 to 1750 Å.

## 4. Models

It was not until recently that population synthesis models accounting for VMS became available. Martins & Palacios (2022) are able to reproduce A1's STIS He II line with a 2 Myr BPASS population synthesis model that accounts for close-binary evolution for stars of up to 100 $M_\odot$, and the added contribution of VMS. However, as shown in their figure 8, their solution results in a poor fit to the N V $\lambda$1240 and C IV $\lambda$1550 stellar wind features.

The COS observations that we use in this work have higher spectral resolution and SNR in the continuum compared to the STIS observation. They also cover a longer wavelength range. We use these higher quality observations to test the most recent Charlot & Bruzual population synthesis models (Plat *et al.* 2019), which account for the contribution of VMS of up to 300 $M_\odot$. The models use the PARSEC stellar evolution tracks of Chen *et al.* (2015), which are for single, non-rotating stars. The tracks take into consideration the formulation of mass loss rates by Vink *et al.* (2011). The model atmospheres and synthetic spectra of the Wolf-Rayet (WR) stars are those of the Potsdam group (PoWR, Gräfener, Hamann, Sander, Shenar, Hainich, Todt et al.). We assume a Simple Stellar Population (SSP), i.e., a single burst of star formation; and exclude the contribution of the ionized gas, as no nebular emission lines are present. We leave the metallicity and age of the stellar population as free parameters. We do not include the reddening due to dust in the model because the comparison with the observation is done in normalized space.

## 5. Main results

Figure 2 shows the comparison between the COS spectrum (blue curve) and our best-fit model with VMS (orange curve). The model has $Z = 0.008$ and age = 2.4 Myr. Note that interstellar absorption lines originating in the Milky Way and NGC 3125-A1 have not been removed from the observations. The model provides a very reasonable fit to the C III $\lambda$1175, N V $\lambda$1240, C IV $\lambda$1550, He II l$\lambda$1640, and N IV $\lambda$1718 photospheric and stellar-wind features, although in the model, the emission component of the C IV P-Cygni like profile is a bit too strong. In addition, O V $\lambda$1371, which can be strong in VMS, is not very well reproduced. Note however that O V is known to be sensitive to clumping in the stellar wind Wofford *et al.* (2014). Overall, our results show the great improvement of stellar evolution and population synthesis models over the past decade, and confirm the importance of including VMS in population synthesis models.

## 6. Discussion

Several of the stellar-wind features that are observed in the COS spectrum of A1 are also observed in the spectra of classical WR stars. However, the presence of a strong O V $\lambda$1371 absorption line in A1's spectrum is an indication that this system is too young to already have classical WR stars. At a metallicity of $Z = 0.008$, classical WR stars start appearing at $\sim$3 Myr and their contribution in a SSP peaks at $\sim$4 Myr. At the age of our best-fit model, which is 2.4 Myr, VMS would still be present. This is why the presence of VMS is the preferred explanation for the observed spectrum of A1.

## 7. Acknowledgments

We thank J. Vink for pointing out that H-rich VMS have WR features, independent of He enrichment. We also thank S. Hernández for helping with the correction of A1's COS spectrum for Lyman-alpha absorption in the Milky Way and NGC 3125, which

https://doi.org/10.1017/S1743921322002502 Published online by Cambridge University Press

was crucial to test if the models fit well the nearby N V $\lambda$1240 stellar-wind doublet. Discussions with P. Crowther and T. Shenar during the conference helped clarify why VMS and not classical WR stars are the main contributors to the UV spectrum of A1.

## References

Bosch, G., Terlevich, E., and Terlevich, R. 2009, *A J*, 137, 3437B
Brands S. A., de Koter, A., Bestenlehner, J. M., *et al.* 2022, *A & A*
Brinchmann, J., Charlot, S., White, S. D. M., *et al.* 2004, *MNRAS*, 351, 1151
Chandar, R., Leitherer, C., Tremonti, C. 2004, *ApJ*, 604, 153
Chen, Y., Bressan, Girardi, L., *et al.* 2015, *MNRAS*, 452, 1068
Crowther, P. A., Schnurr, O., Hirschi, R. *et al.* 2010, *MNRAS*, 408, 731
Eldridge, J. J., Stanway, E. R., Xiao, *et al.* 2017, *PASA*, 34, 58E
Hadfield, L. J., Crowther, P. A. 2006, *MNRAS*, 368, 1822
Martins, F., Palacios, A. 2022, *A & A*, 659, 163
Plat, A., Charlot, S., Bruzual, G., *et al.* 2019, *MNRAS*, 490, 978
Saxena, A., Pentericci, L., Mirabelli, M. *et al.* 2020, *A & A*, 636, 47
Shapley, A., Steidel, C. C., Pettini, M., *et al.* 2003, *ApJ*, 588, 65S
Vink, J. S., Muijres, L. E., Anthonisse, B., *et al.* 2011, *A & A*, 531A, 132V
Wofford, A., Leitherer, C., Chandar, R., *et al.* 2014, *ApJ*, 781, 122